International Journal of Fatigue 165 (2022) 107162

Contents lists available at ScienceDirect

International Journal of Fatigue

journal homepage: www.elsevier.com/locate/ijfatigue

The effects of welded clips on fatigue crack growth in AA6156 T6 panels

Aleksandar Sedmak [a,*], Aleksandar Grbovic [a], Blagoj Petrovski [b], Abulgasem Sghayer [a], Simon Sedmak [b], Filippo Berto [c], Andrijana Đurđević [d]

[a] Faculty of Mechanical Engineering, University of Belgrade, Kraljice Marije 16, 11000 Belgrade, Serbia
[b] Innovation Center of the Faculty of Mechanical Engineering, Kraljice Marije 16, 11000 Belgrade, Serbia
[c] Faculty of Engineering, NTNU, Richard Birkelands vei 2b, 7491 Trondheim, Norway
[d] Academy of Applied Technical Sciences, Belgrade, Serbia

A B S T R A C T

Fatigue crack growth in different panels, made of AA6156 T6, was investigated experimentally and numerically. Three different types of panels were used, simple one, so-called base metal (BM), panel with 4 welded stringers and panel with 4 welded stringers and 3 welded clips. Experimental investigation indicated benefits of stringers, especially in respect to residual life, since the number of cycles were more than doubled (420 Kcyc vs 195 Kcyc for initial crack length 14 mm), but that was not the case for panels with clips (220 Kcyc). Experimental investigation was also performed on panels with longer cracks (75 mm) to check the effect of initial crack length in the case of BM and panels with 4 stringers, showing practically the same effect of stringers on residual life (95 Kcyc vs 50 Kcyc). Then, fatigue crack growth in panels was simulated numerically using xFEM. Numerical simulation indicated the same trend and effectiveness of stringers, with sufficient agreement with experimental results for BM and panels with stringers only. Anyhow in the case of clips panels with 4 stringers and 3 clips, number of cycles for panel with additional 3-clips was higher than for panel with just 4-stringer, (278 Kcyc vs 265 Kcyc), improving fatigue life for cca 5 %, contrary to experimental results.

1. Introduction

Riveting has been the state of the art joining technology in the aeronautical industry for decades and it has demonstrated its value and reliability. But the necessary overlap joint demands large amounts of material and its production chain is also time consuming. New processes such as Laser Beam Welding (LBW) and Friction Stir Welding (FSW) present new solutions to overall weight savings and process time reduction, [1,2]. These processes are continuously under improvement and their application is still to be broadened. It has been observed in larger metallic structures of models such as in the A318, A340 and A380 that LBW has advantages compared to conventional riveted fuselages. Regarding the production of structures, LBW can be up to 20 times faster than riveting. Another advantage is that the process only requires one-sided access. Lower fuselage panels made of AA6xxx series (Al-Mg-Si-Cu) and processed with LBW as an efficient joining technology are already established in the market, Fig. 1.

Although LBW has been successfully applied for manufacturing skin-stringer panels, as shown in Fig. 2a, two types of cracks appeared in a large transport aircraft, longitudinal cracks due to hoop stresses and circumferential cracks due to bending of the fuselage, [4], because not all welds are sound, as shown Fig. 2b, even though the microstructure was practically the same, i.e. typical for LBW. Thus, it is of utmost importance to predict fatigue crack growth rate. Extensive experimental study has been performed in GKSS, [5], using different panels, Fig. 3, followed by recent numerical simulation using xFEM, [3,6–9]. Two different ways of improving panel performance were analysed, focused on the effect of stringers only and stringers and clips together, [6–9].

The most common method for numerical simulation of FCG nowadays is the extended FEM (xFEM), introduced in nineties by Ted Belytschko and his coworkers, [10,11] and modified later on, [12]. Its effectiveness for FCG simulation has been demonstrated in number of applications, not only for welded joints, as shown in [13–20], but also for other, completely different problems, like artificial hips and biomaterials in general, [21–23]. As closely related to the problem analysed here, one should keep in mind fatigue life analysis of the integral skin-stringer panel using xFEM, [3], numerical simulation of fatigue crack propagation in friction stir welded joint made of Al 2024-T351 alloy, [13], stringer effect on fatigue crack propagation in A2024-T351 aluminum alloy welded joint [6], experimental and numerical analysis of fatigue crack growth in integral skin-stringer panels, [7], application of xFEM for fatigue life predictions of multiple site damage in aircraft structure, [14], fatigue life estimation of damaged integral wing spar using xFEM, [15], fatigue life estimation of CCT specimen using xFEM and Paris law, [16], all of them briefly described in [17]. One should also keep in mind other investigations of FCG in stiffened and plain panels by classical fracture mechanics approach, [24–25], where stress intensity

* Corresponding author.
E-mail address: asedmak@mas.bg.ac.rs (A. Sedmak).

https://doi.org/10.1016/j.ijfatigue.2022.107162
Received 28 January 2022; Received in revised form 20 May 2022; Accepted 19 July 2022
Available online 22 July 2022

Nomenclature

LBW	Laser Beam Welding
FSW	Friction Stir Welding
FCG	Fatigue Crack Growth
DIC	Digital Image Correlation
xFEM	extended Finite Element Method
P+4S	Panel with 4 stringers
P+4S+3C	Panel with 4 stringers and 3 clips
δ_5	crack tip opening displacement
a	crack length
a_0	initial crack length
W	plate width
Kcyc	1000 cycles
N	Number of cycles
da/dN	Fatigue Crack Growth rate
ΔK	stresss intensity factor range
BM	Base Metal
HAZ	Heat-Affected-Zone

factors were calculated by FEM and fatigue life was assessed by integrating the Paris equation, as well as similar approach used to assess residual stress effects, [26–27]. Significant difference should be noticed between use of FEM and xFEM for FCG simulation, since in the former case mesh has to be adapted in each step, whereas xFEM does not require mesh change. Anyhow, nowadays automatic mesh adaption is available, making standard FEM competitive with xFEM, [28].

2. Experimental research

Extensive experimental research was performed in GKSS [5], including testing of residual strength, Crack Tip Opening Displacement, δ_5 and J-R curves, using Digital Image Correlation (DIC), and monitoring of fatigue crack growth (FCG). In this paper, the focus is on monitoring of FCG during testing of 4-Stringer Flat Panels made of AA6156 T6, 2 W = 760 mm, with or without 3 clips, as shown in Fig. 4. Digital Image Correlation was used to measure the crack tip opening displacement, δ_5, as explained in detail in [29–32] and shown in Fig. 5. The average maximum force was $F_{max} = 112.954$ KN, while the load ratio R = 0.146 was determined on the basis of average minimum tensile force measured. Load frequency was 2 Hz.

Clip with a crack is schematically presented in Fig. 6, whereas its appearance after panel failure is given in Fig. 7, indicating crack growth not retarded by clips, which is in agreement with experimental results to be presented later.

Comparison of FCG in Base Metal (BM) and LBW Panels is presented in Figs. 8 and 9. In Fig. 8 the left tip of crack is analysed in terms of FCG rate, da/dN, vs crack length, a, for BM and both panels, one with 4 stringers (referred to as P+4S from now on), and the other one with 3 clips, in addition (referred to as P+4S+3C). One should keep in mind that the initial crack length was not the same in all three cases, since it was $2a_0 = 14$ mm for BM and P+4S+3C, while $2a_0 = 75$ mm for P+4S. Therefore, more relevant is comparison between BM and P+4S+3C. One

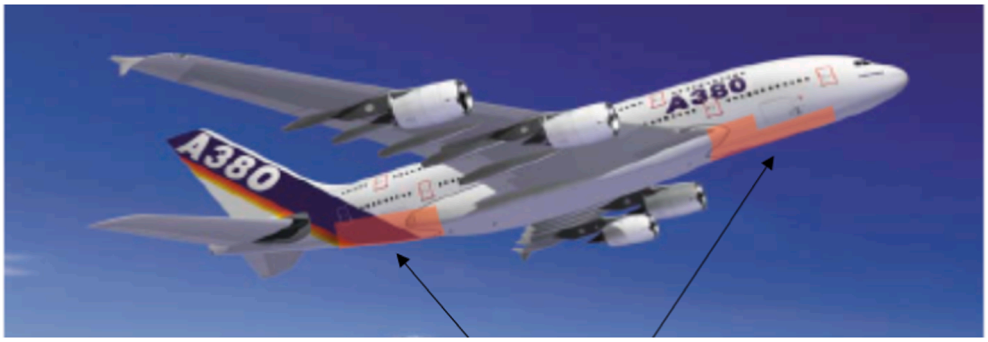

Fig. 1. LBW panels (in orange) in A380. (For interpretation of the references to colour in this figure legend, the reader is referred to the web version of this article.)

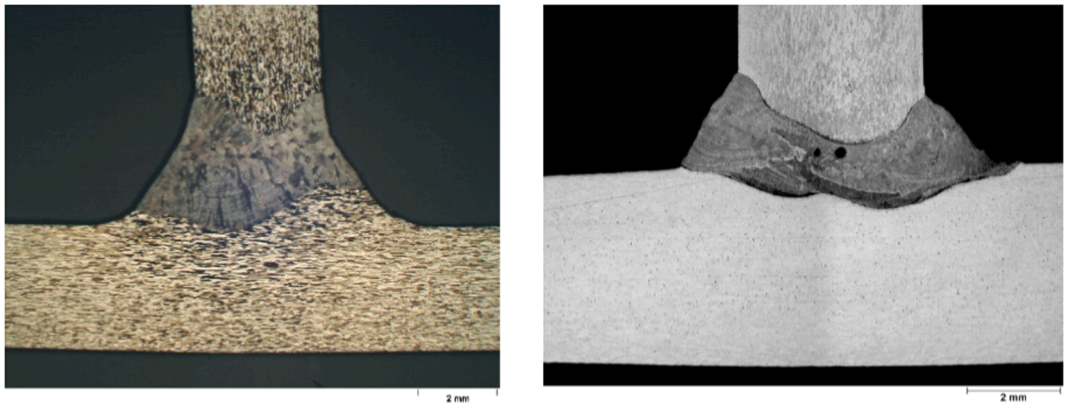

Fig. 2. LBW joints, a) no defects, b) large pores.

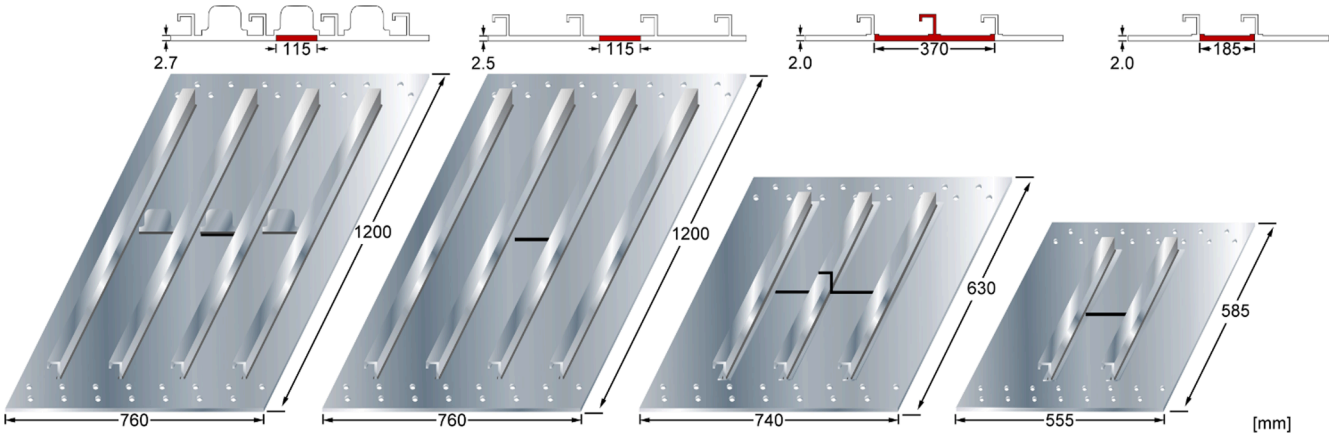

Fig. 3. Panels welded by LBW with different number of stringers and clips.

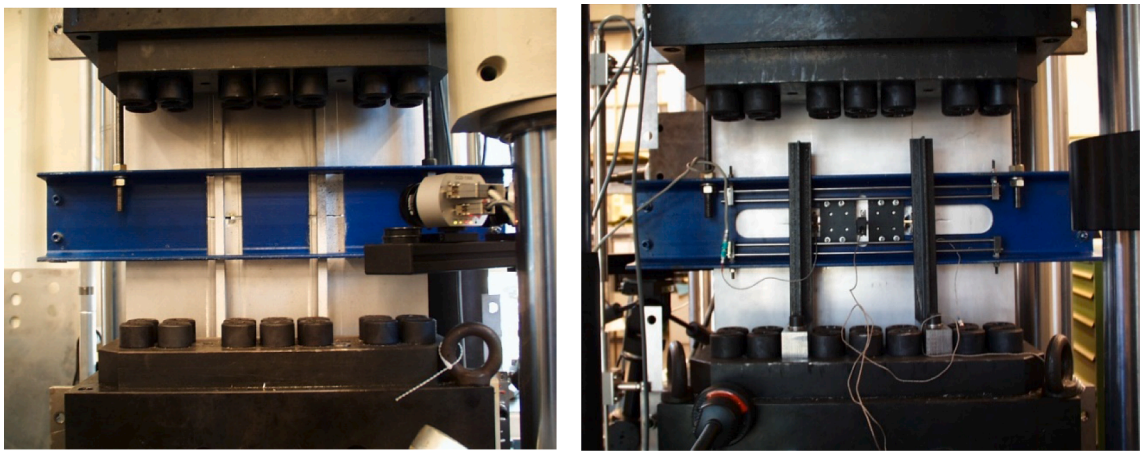

a) Panel in testing position, b) FCG monitoring

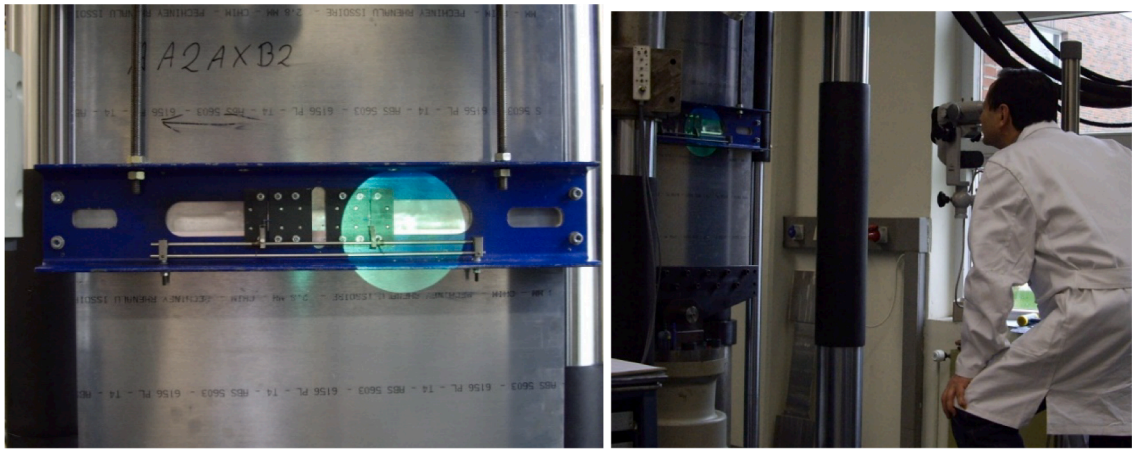

c) Region of DIC monitoring d) DIC monitoring

Fig. 4. Testing of panels.

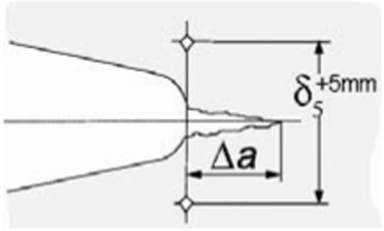

Fig. 5. CTOD (δ_5) reference points for measurement by DIC.

can see that FCG rates are similar when crack is growing along both clips, middle and left, whereas in between there is a significant slow-down at the end on the middle clip, followed by slower crack growth up to the left clip. Once crack reached the left clip, FCG rate is significantly increased, closing up with the rate in BM. One can argue that clips are only helpful in combination with stringer, while on their own they do not act as a barrier to crack growth, probably because crack is growing along Heat-Affected-Zone (HAZ). Behaviour of a longer crack in P+4S is somewhat different, but basically the same, speeding up until the end of middle clip, slowing down up to the stringer and again, speeding up once the left clip is reached, but at a somewhat smaller rate. Similar behaviour can be also observed for the right crack tip, with slightly different pattern of crack growth in P+4S+3C, Fig. 9.

More details about crack growth in P+4S+3C are given in Fig. 10a in form of diagramme a vs N, and in Fig. 10b, showing comparison of a vs N for BM and P+4S+3C, with somewhat longer life in the latter case (225 Kcyc vs 193 Kcyc).

More details about crack growth in P+4S are given in Fig. 11, in form of results for FCG rate, da/dN, vs stress intensity factor range, ΔK, Fig. 11a, and crack length, a, vs number of cycles, N, for both P+4S and BM, for comparison purpose, Fig. 11b. One can see that the FCG is slowed down due to stiffener effect, making the residual life of P+4S significantly longer than BM.

In order to check a possible effect of crack length, additional testing was done on plates with $2a_0 = 75$ mm, both for BM and P+4S. Diagram in Fig. 12 shows crack length, a, vs number of cycles, N, for the initial crack length $2a_0 = 75$ mm, indicating N close to 100 Kcyc for crack length $2a = 230$ mm. Also, one can see that after 67 Kcyc crack started to grow through stringer, as well, reaching length 120 mm after 95 Kcyc. Comparison of crack length, a, vs number of cycles, N, is given in Fig. 13, indicating significant increase in residual life of P+4S, especially if loading is applied on stringers (50, 78, 95 Kcyc for BM, skin loaded and stringer loaded P+4S, respectively). In this way we have also verified the comparison given in Figs. 8 and 9, where different initial crack lengths were used for BM and P+4S+3C ($2a_0 = 14$ mm) and P+4S ($2a_0 = 75$ mm).

3. Numerical simulation of fatigue crack growth

Numerical simulation of panels by using xFEM has been presented in more details in [8,9,33], whereas here only the most important results and findings will be shown for AA6156 T6 and crack length $2a = 14$ mm. To start with, Fig. 14 presents comparison between the experimental and numerical results for AA6156 T6 BM, indicating good agreement, as well as conservative approach of xFEM, [8]. The maximum force was Fmax = 112.95 KN, while the load ratio R = 0.146 was determined on the basis of average minimum tensile force. Coefficients in Paris law, m = 3.174 and C = 1.772E-12 were determined in previous experimental research, as explained in [5–9]. Units are defined in accordance with Paris law, $da/dN = C(\Delta K)^m$, with a in mm and ΔK in MPa$\sqrt{m}$.

One important issue covered in [8,9] was about the effect of FE mesh size. Three different sizes were used, 1 mm, 2 mm (two options, with toe modelling and without it) and 4 mm, to evaluate FCG in P+4S, Fig. 15. One can see that the finest mesh size predicts the lowest number of cycles, while meshes with 2 mm and 4 mm are in good mutual

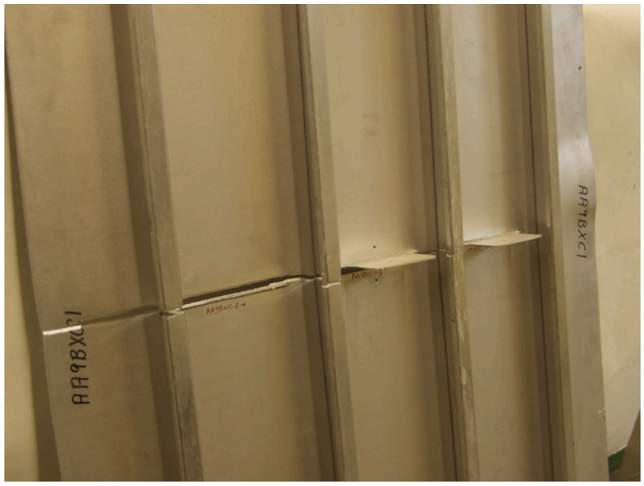

Fig. 7. Panel with 4 stringers and 3 clips after failure.

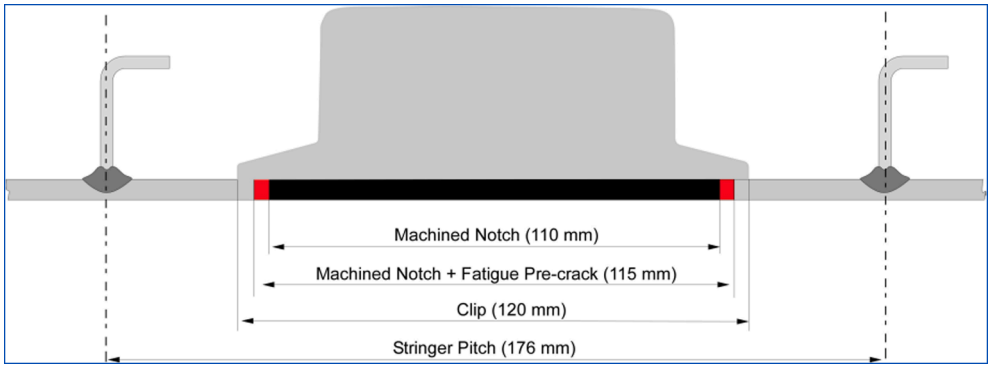

Fig. 6. Schematic presentation of the clip in a panel.

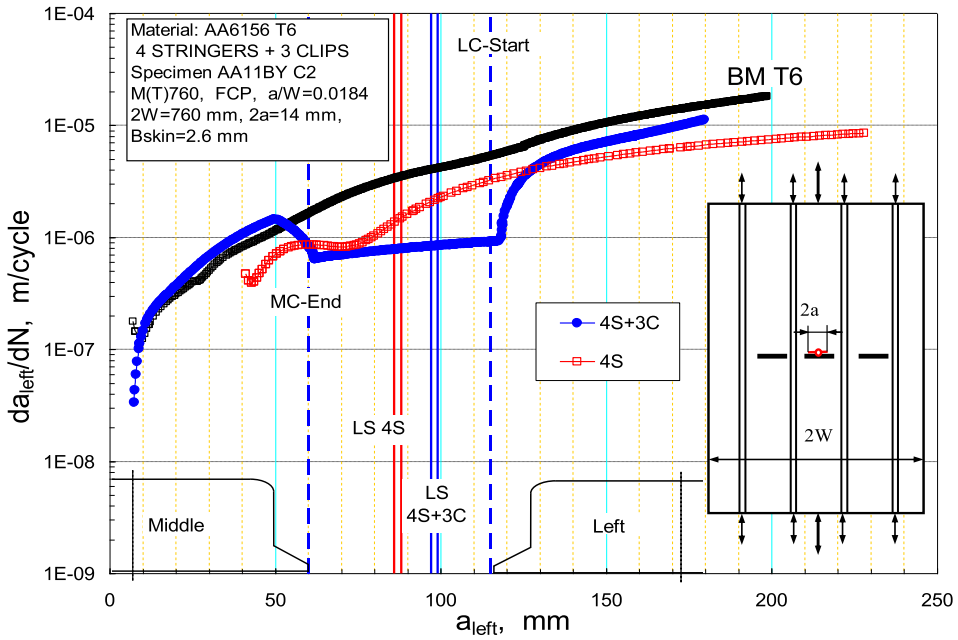

Fig. 8. Fatigue Crack Growth rate vs crack "left" length, $2a_0 = 14$ mm (blue), $2a_0 = 75$ mm (red). (For interpretation of the references to colour in this figure legend, the reader is referred to the web version of this article.)

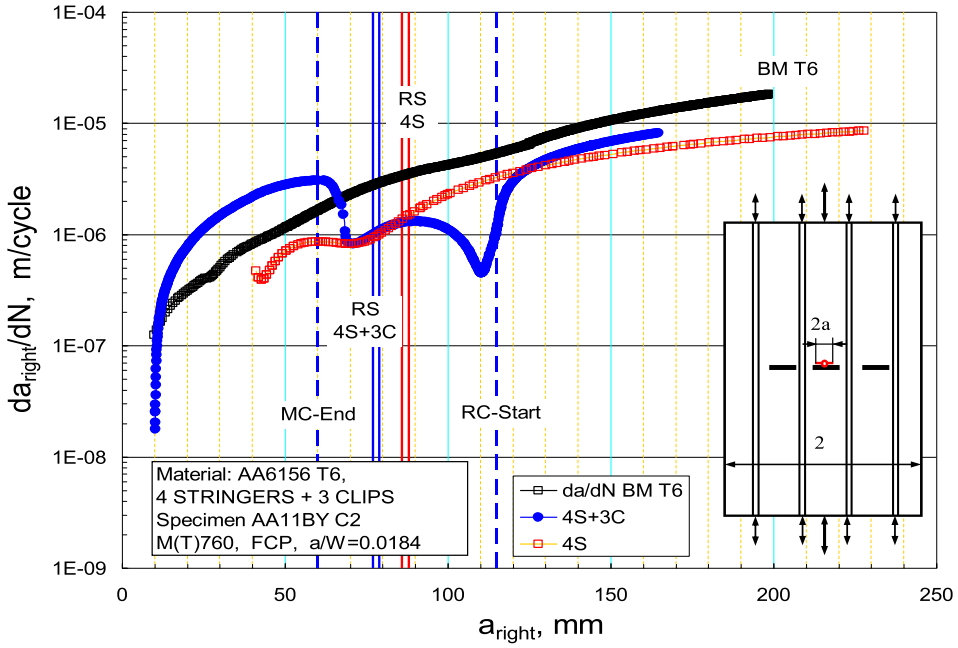

Fig. 9. Fatigue Crack Growth rate vs crack "right" length, $2a_0 = 14$ mm (blue), $2a_0 = 75$ mm (red). (For interpretation of the references to colour in this figure legend, the reader is referred to the web version of this article.)

agreement (N close to 300 Kcyc), but still rather conservative compared to the experimental results (420 Kcyc). This issue is still open, since numerical prediction is a bit too conservative. One should also notice that different properties in different welded joint zones were not taken into account in this analysis.

Figs. 16 and 17 present two characteristic crack growth moments, after 60th and 117th steps for mesh 2 mm, and 88th and 278th for mesh 4 mm. Since the appearance of crack growth looks more realistic for the mesh 2 mm, this one was chosen for modelling of P+4S+3C.

The P+4S+3C was modelled with mesh 2 mm, in the same way as in the case of P+4S. Crack was propagated in 91 steps, with 2 mm increments in each step. After 14 steps, as shown in Fig. 18a, the first clip began to deform along its length. At the same time, crack continued to grow through the base metal plate, along the weld, reaching the wall of the right and left stringer after 91 steps, Fig. 18b, and starting to grow also through the stringers. One should notice that clip is practically not deformed, contrary to stringers, making important difference, since it reflects on the number of cycles and life of the panel.

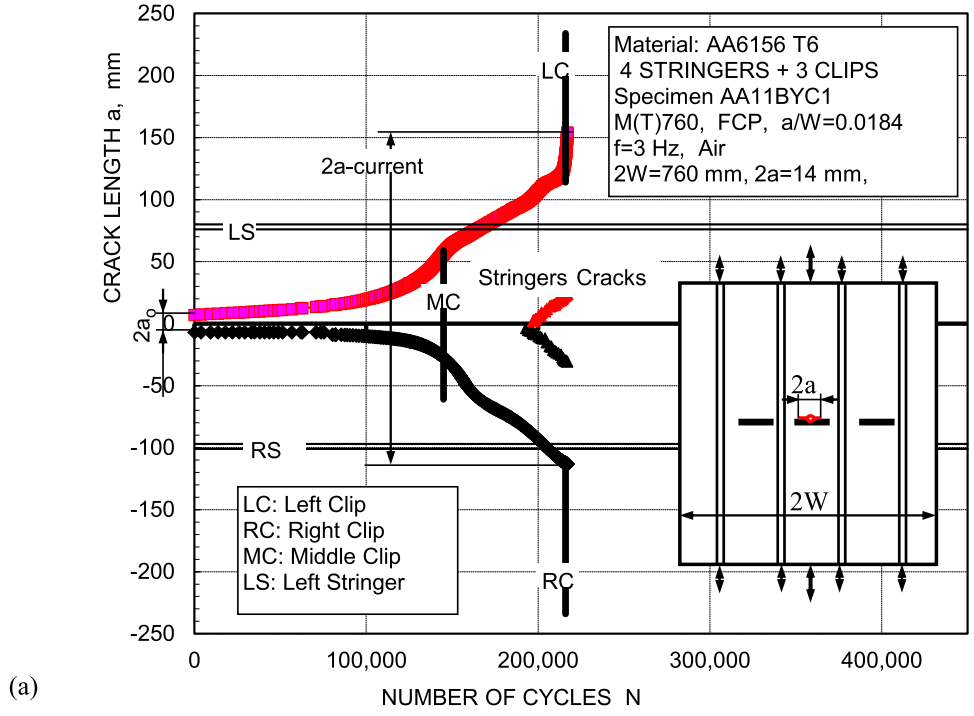

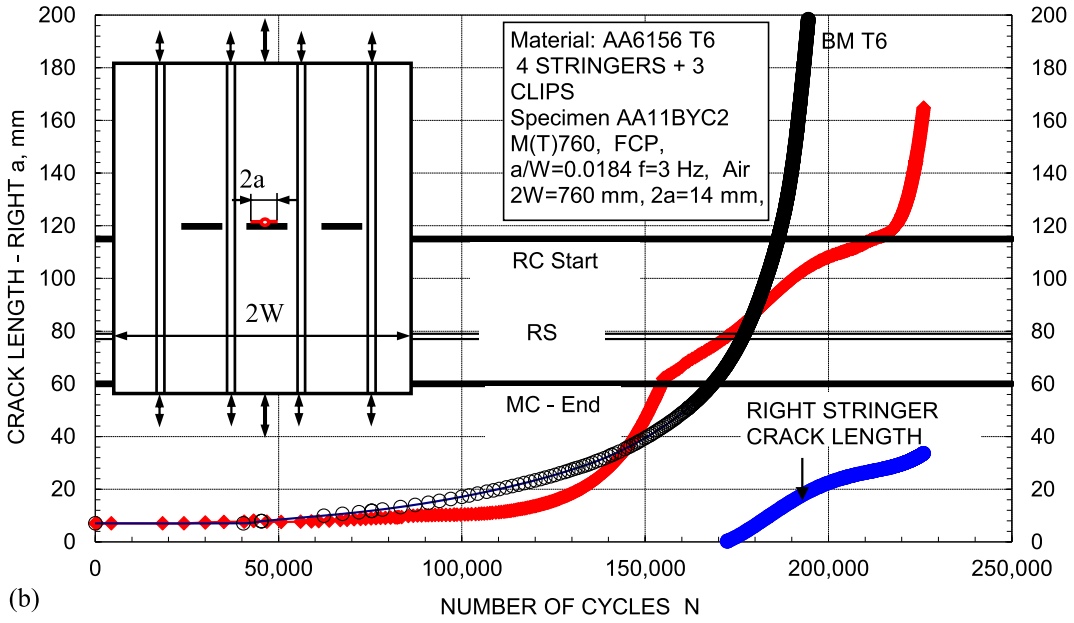

Fig. 10. Crack length a vs number of cycles N, a) P+4S+3C, b) Comparison BM and P+4S+3C.

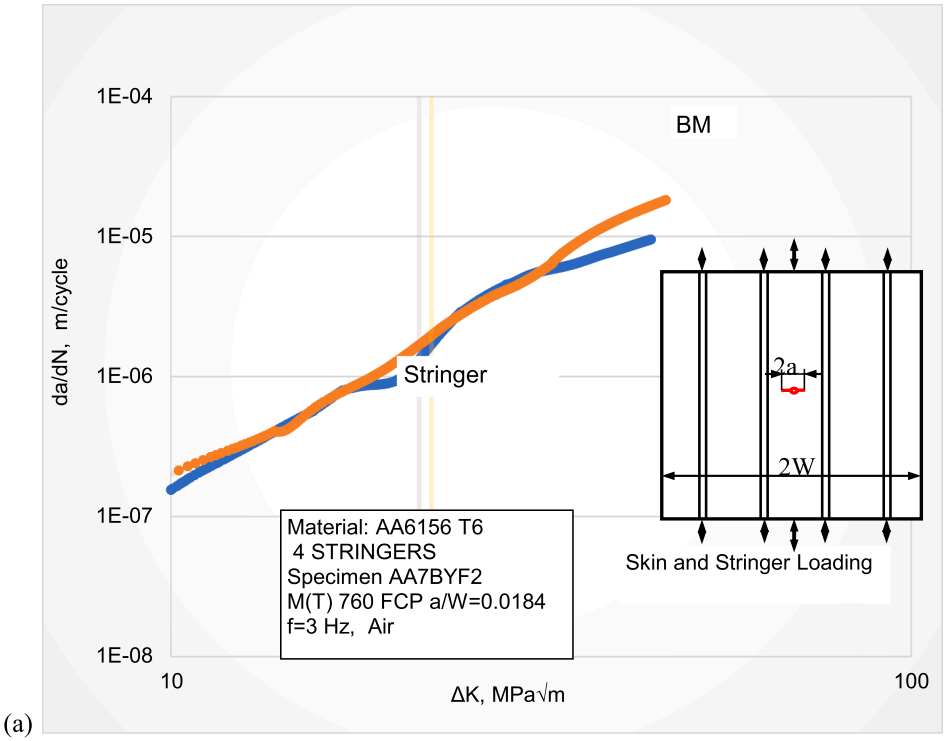

Fig. 11. Comparison of BM and P+4S+3C, a) FCG rate vs stress intensity factor range, b) Crack length vs number of cycles.

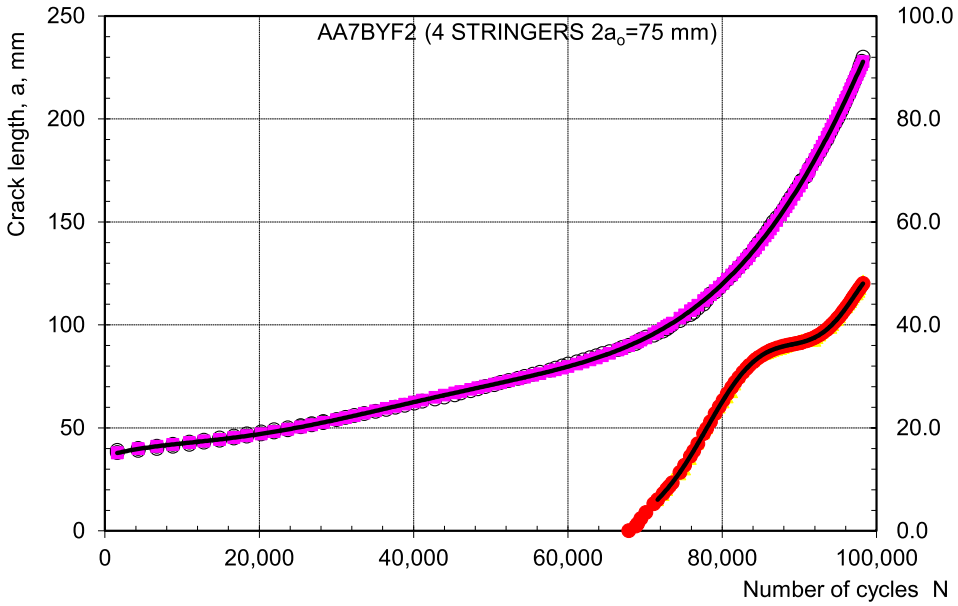

Fig. 12. Crack length vs number of cycles for the initial crack length $2a_0 = 75$ mm.

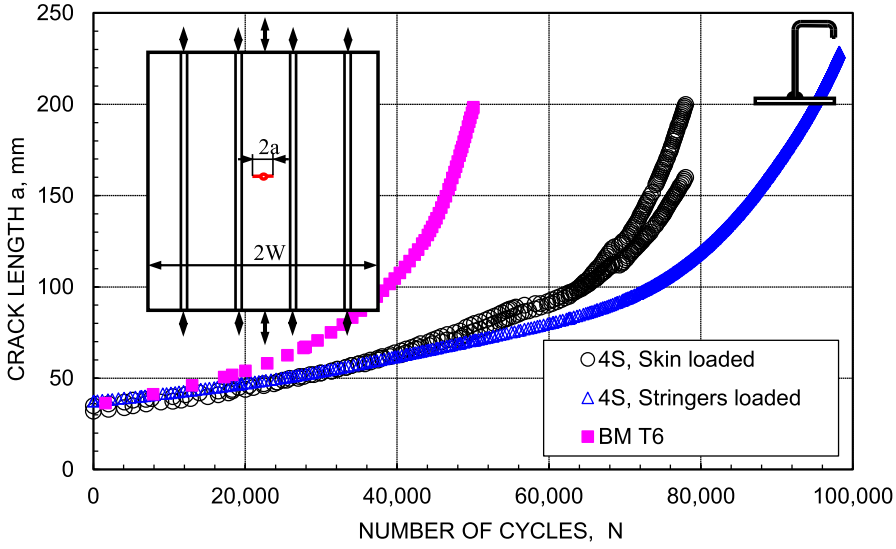

Fig. 13. Crack length vs number of cycles for BM and P+4S, loaded via stringer and skin.

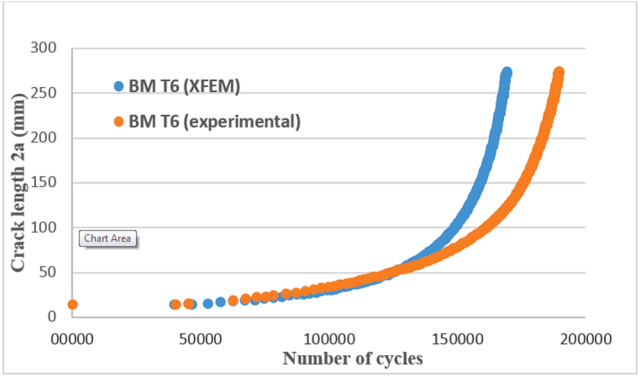

Fig. 14. Numbers of cycles obtained in experiment and xFEM simulation (base metal T6), [8].

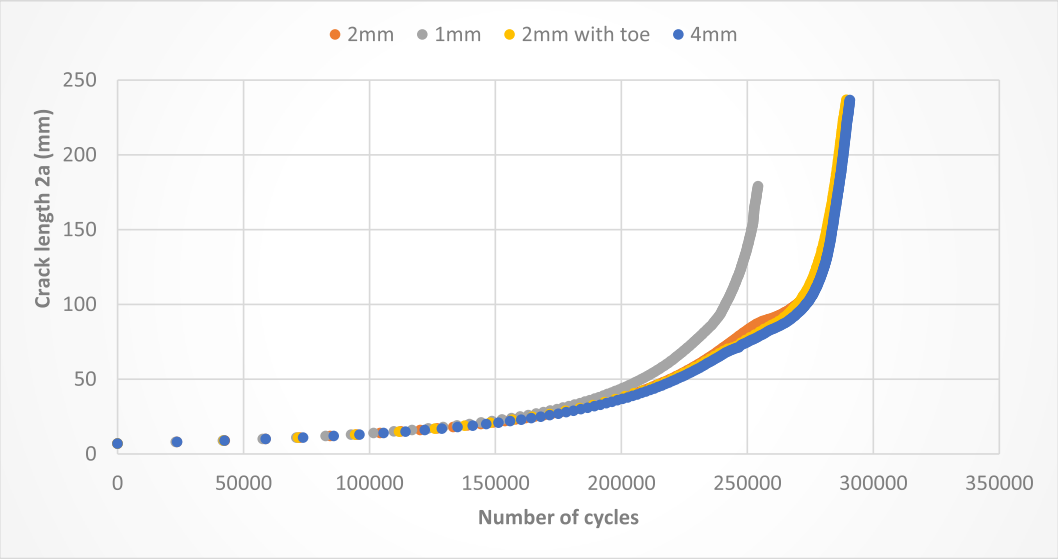

Fig. 15. Crack length vs number of cycles for P+4S, different mesh sizes, [9].

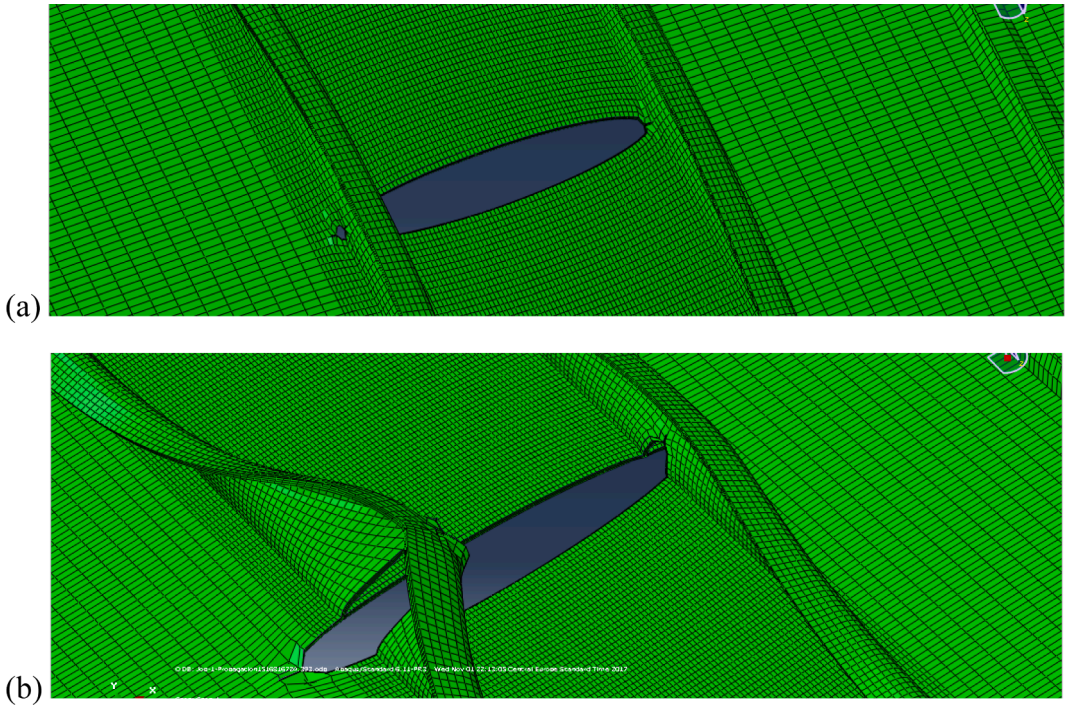

Fig. 16. Mesh 2 mm: a) 60 steps, crack begins to spread along the stringer, b) 117 steps, first and second stringers are damaged, [9].

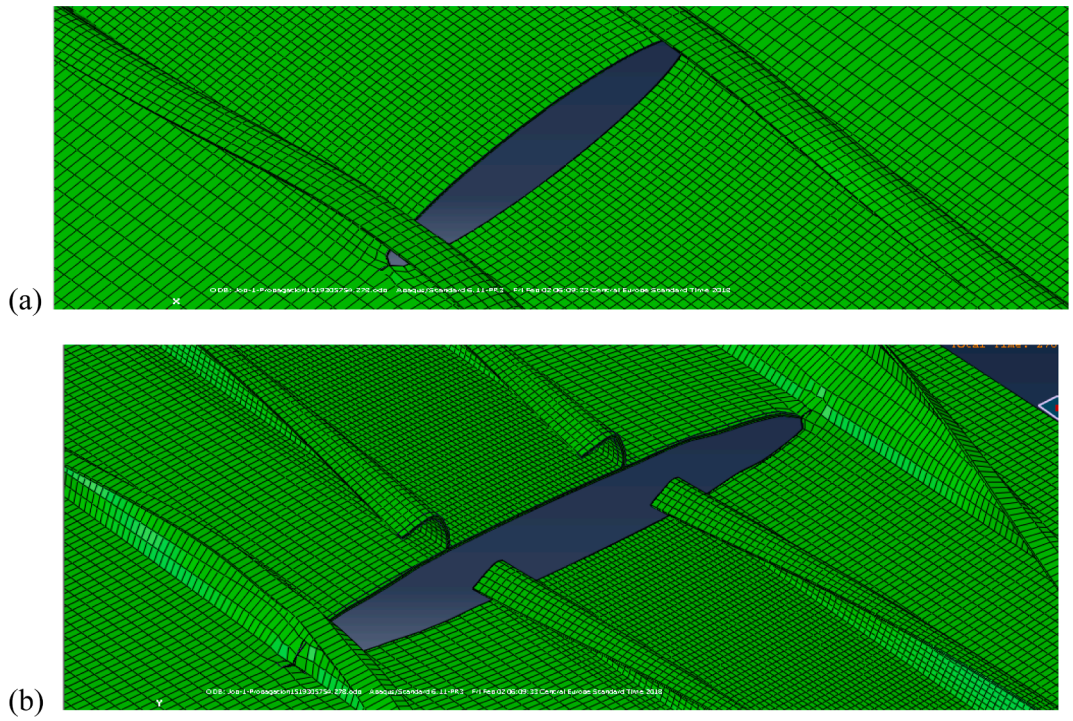

Fig. 17. Mesh 4 mm: a) 88 steps, crack begins to spread along the stringer, b) 278 steps, third and fourth stringers are damaged, [9].

Results for crack length vs number of cycles are shown in Fig. 19, as a comparison between P+4S and P+4S+3C. One can see that the number of cycles for panel with additional 3-clips is higher than for panel with just 4-stringer, (278,476 cycles vs 264,958) cycles, improving fatigue life for just 5 %. One should also notice that P+4S+3C is performing somewhat better than P+4S, which can be explained by the fact that numerical simulation did not take into account HAZ effects, which are dominant in the plate with clips, as shown in experimental analysis. Anyhow, the life improvement obtained by clips does not justify complicated and expensive production of panels with clips.

4. Discussion

Following aspects of the investigation of fatigue crack growth in different panels are now discussed:

- The effect of stringers on residual life of panels.
- The effect of initial crack length.
- How well xFEM can simulate FCG?
- Why welded clips seemingly do not work?

Experimental results clearly indicated significantly longer life of panel with stringers, since the number of cycles were more than doubled (420 Kcyc vs 195 Kcyc for initial crack length 14 mm), but not in the case for panels stringers and clips (220 Kcyc). The most probable reason for this unexpected result is low resistance to crack growth of HAZ due to its unfavourable microstructure after LBW.

Testing of BM and panels with 4 stringers with longer cracks (75 mm) confirmed the effectiveness of stringers in prolonging panel life, almost 2 times (95 Kcyc vs 50 Kcyc), similar to the “short” crack case (14 mm).

Numerical simulation by xFEM provided good agreement with the experimental results for BM and panels with stringers only, as shown in detailed analysis given elsewhere [7,9]. Contrary to that, in the case of clips panels with 4 stringers and 3 clips, number of cycles was higher than for panel with just 4-stringer, (278 Kcyc vs 265 Kcyc) cycles, improving fatigue life for cca 5 %, whereas experimental results indicated significantly shorter life (225 Kcyc vs 420 Kcyc). Most probably, this is caused by the fact that HAZ was not modelled, so the crack was growing through the base metal (along the welded joint), which presumably has much higher crack growth resistance.

As already explained, both experimental and numerical results indicate that HAZ is the most probable cause of the fact that welded clips failed to improve panel residual life. One can argue that LBW, used here to weld clips and panel, produces unfavourable properties of HAZ due to its high energy, being otherwise significant advantage of a welding process. Also, one should keep in mind that stringer welded joints are perpendicular to crack growth, whereas crack grows in direction of clips welded joints. In other words, it is not justified to increase production costs with additional welding of 3 clips, even if some beneficial effect (as predicted by xFEM, but to small extent) is obtained.

5. Conclusions

Based on the results presented in this paper, one can conclude the following:

1. Stringers significantly increase life of a panel, since the number of cycles were more than doubled (420 Kcyc vs 195 Kcyc for initial crack length $2a_0 = 14$ mm and 95 Kcyc vs 50 Kcyc for $2a_0 = 75$ mm).
2. Clips failed to do the same (220 Kcyc for initial crack length $2a_0 = 14$ mm) presumable due to low resistance to the crack growth of HAZ, which presumably was the region of crack growth.
3. Numerical simulation by xFEM provided good agreement with the experimental results for BM and panels with 4 stringers, but not for panels with 4 stringers and 3 clips, due to the fact that HAZ was not modelled, enabling unrealistic crack growth through the region of higher crack growth resistance.

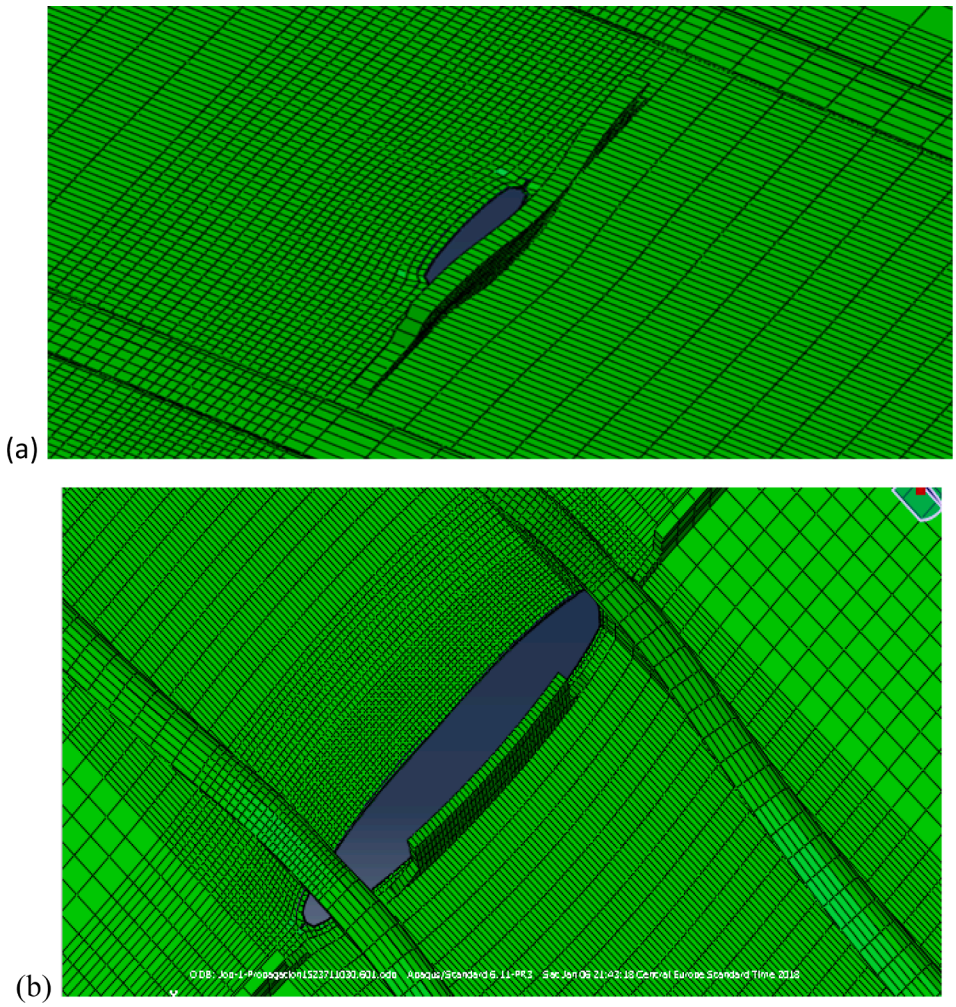

Fig. 18. Central crack: a) 14 steps, b) after 91 steps of growth, [9,33].

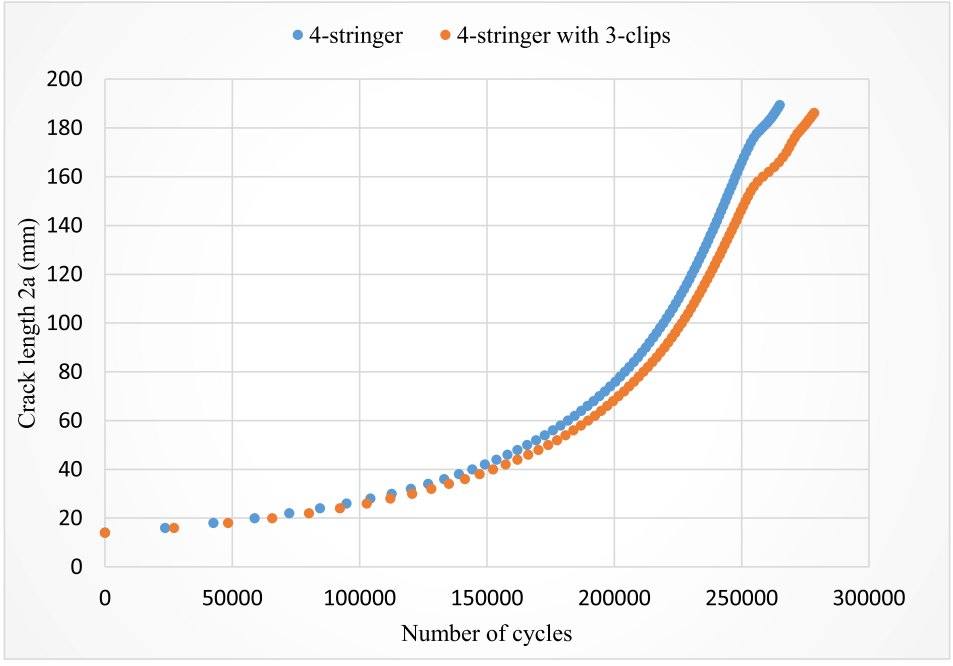

Fig. 19. Crack length vs number of cycles for P+4S and P+4S+3C [33].

Declaration of Competing Interest

The authors declare the following financial interests/personal relationships which may be considered as potential competing interests: Aleksandar Sedmak reports financial support was provided by Republic of Serbia Ministry of Education Science and Technological Development..

Acknowledgements

This research was supported by the Ministry of Sciences and Technology of Republic of Serbia through the contracts 451-03-9/2021-14/200105 and 451-03-9/2021-14/200213.

References

[1] Bayraktar FS. Analysis of residual stress and fatigue crack propagation behaviour in laser welded aerospace aluminium T-joints. Technischen Universität Hamburg; 2011. PhD thesis.
[2] Braun R, Dalle-Donne C, Staniek G. Laser beam and friction stir welding of 6013–T6 aluminium alloy sheet. Material-wissenschaft und Werkstofftechnik 2000; 31(12):1017–26.
[3] Sghayer A, Grbović A, Sedmak A, Dinulović M, Doncheva E, Petrovski B. Fatigue life analysis of the integral skin-stringer panel using XFEM. Structural Integrity and Life 2017;17:7–10.
[4] Venkatesha BK, Suresh BS, Girish KE. Analytical evaluation of fatigue crack arrest capability in fuselage of large transport aircraft. Int J Theoret Appl Res Mech Eng 2012;1(1):13–22.
[5] Koçak M, Petrovski B, Palm VF, Kocik R, Syassen F. Damage Tolerance Analysis of Laser Beam, Welded Short Distance Clip Welds using 4-Stringer Flat Panels. European Workshop on Short Distance WELding Concepts for AIRframes - WELAIR, GKSS Research Center, Geesthacht (Hamburg) – Germany, 13-15 June 2007.
[6] Kraedegh A, Sedmak A, Grbovic A, Sedmak S. Stringer effect on fatigue crack propagation in A2024–T351 aluminum alloy welded joint. Int J Fatigue 2017;105: 276–82.
[7] Sghayer A, Grbović A, Sedmak A, Dinulović M, Grozdanović I, Sedmak S, et al. Experimental and Numerical Analysis of Fatigue Crack Growth in Integral Skin-Stringer Panels. Technical gazette 2018;25(3):785–91.
[8] Grbović A, Sedmak A, Kastratović G, Petrašinović D, Vidanović N, Sghayer A. Effect of laser beam welded reinforcement on integral skin panel fatigue life. Eng Fail Anal 2019;101:383–93.
[9] Sghayer A. Fatigue life assessment of damaged integral skin–stringer panels, Doctoral thesis, Faculty of Mechanical Engineering. University of Belgrade; 2018.
[10] Belytschko T, Lu YY, Gu L. Element-free Galerkin methods. Int J Numer Methods Eng 1994;37(2):229–56.
[11] Babushka I, Melenk JM. The partition of unity method. Int J Numer Methods Eng 1998;40(4):727–58.
[12] Jovičić G, Živković M, Sedmak A, Jovičić N, Milovanović D. Improvement of algorithm for numerical crack modeling. Archives Civil Mech Eng 2010;10(3): 19–35.
[13] Djurdević A, Živojinović D, Grbović A, Sedmak A, Rakin M, Dascau H, et al. Numerical simulation of fatigue crack propagation in friction stir welded joint made of Al 2024–T351 alloy. Eng Fail Anal 2015;58:477–84.
[14] Rakipovski E, Grbović A, Kastratović G, Vidanović N. Application of Extended Finite Element Method for Fatigue Life Predictions of Multiple Site Damage in Aircraft Structure. Struct Integrity Life 2015;15(1):3–6.
[15] Eldwaib K, Grbović A, Sedmak A, Kastratović G, Petrasinović D, Sedmak S. Fatigue Life Estimation of Damaged Integral Wing Spar Using XFEM. Technical Gazette 2018;25(6):1837–42.
[16] Eldwaib KA, Grbovic A, Kastratovic G. Fatigue Life Estimation of CCT Specimen Using XFEM and Paris Law. Struct Integrity and Life 2017;17(2):117–24.
[17] Sedmak A. Computational fracture mechanics: An overview from early efforts to recent achievements. Fatigue Fract Eng Mater Struct 2018;41(12):2438–74.
[18] Kraedegh A, Li W, Sedmak A, Grbovic A, Trišović N, Kirin S. Simulation of fatigue crack growth in A2024–T351 "T" welded joint. Struct Integrity Life 2017;17(1): 3–6.
[19] Zaidi R, Sedmak A, Kirin S, Grbovic A, Li W, Lazic Vulicevic L, et al. Risk assessment of oil drilling rig welded pipe based on structural integrity and life estimation. Eng Fail Anal 2020;112:104508. https://doi.org/10.1016/j.engfailanal.2020.104508.
[20] Đurđević A, Živojinović D, Grbović A, Sedmak A, Rakin M, Dascau H, et al. Numerical simulation of fatigue crack propagation in friction stir welded joint made of Al 2024–T351 alloy. Eng Fail Anal 2015;58(2):477–84.
[21] Colic K, et al. Numerical simulation of fatigue crack growth in hip implants. Procedia Eng 2016;149:229–35.
[22] Sedmak A, Vučetić F, Čolić K, Grbović A, Bozić Ž, Sedmak S, et al. Fatigue crack growth in locking compression plates. Int J Fatigue 2022;157:106727. https://doi.org/10.1016/j.ijfatigue.2022.106727.
[23] Vucetic F, Colic K, Grbovic A, Radakovic Z, Sedmak S. Extended FEM analysis of fatigue crack growth in Ti-6Al-4V orthopaedic plates. Procedia Struct Integrity 2020;28(3):555–60.
[24] Božić Ž, Bitunjac V, Semenski D. Interaction Modelling of Multiple Fatigue Cracks in Stiffened Panels. Trans FAMENA 2010;34(4):11–9.
[25] Božić Ž, Wolf H, Semenski D. Fatigue Growth of Multiple Cracks in Plates under Cyclic Tension, Transactions of FAMENA 2010; 34(1): 1 - 12.Gubeljak, N., Application of stereometric measurement on structural integrity, Structural Integrity and Life, 2006;6(1-2):65–74.
[26] Božić Ž, Schmauder S, Wolf H. The effect of residual stresses on fatigue crack propagation in welded stiffened panels. Eng Fail Anal 2018;88:346–57. https://doi.org/10.1016/j.engfailanal.2017.09.001.
[27] Božić Ž, Schmauder S, Mlikota M, Hummel M. Multiscale fatigue crack growth modelling for welded stiffened panels. Fatigue Fract Engng Mater Struct 2014;37 (9):1043–54.
[28] Schöllmann M, Fulland M, Richard HA. Development of a new software for adaptive crack growth simulations in 3D structures. Eng Fract Mech 2003;70(2): 249–68. https://doi.org/10.1016/S0013-7944(02)00028-0.
[29] Gubeljak N. Application of stereometric measurement on structural integrity. Struct Integrity and Life 2006;6(1–2):65–74.
[30] Vasco-Olmo JM, Díaz FA, Antunes FV, James MN. Characterisation of fatigue crack growth using digital image correlation measurements of plastic CTOD. Theor Appl Fract Mech 2019;101:332–41.
[31] Samadian K, Hertelé S, De Waele W. Measurement of CTOD along a surface crack by means of digital image correlation. Eng Fract Mech 2019;205:470–85.
[32] Patil AB, Toppo SP, Singh RKP. Digital Image Correlation (DIC) Technique for Fatigue Crack Growth Analysis Using ΔCTOD Criteria. Int J Eng Technol 2018;7: 1362–4.
[33] Grbovic A, Sedmak, Petrovski B, Sghayer A, Sedmak S, Razavi J, Berto F. Effect of welded clips on fatigue crack growth in AA6156 T6 panels, Structural Integrity Procedia, 2022;39:786-791.